

The role of silver on the stabilization of the incommensurately modulated structure in calaverite, AuTe_2

LUCA BINDI,^{1,*} ALLA ARAKCHEEVA,² AND GERVAIS CHAPUIS²

¹Museo di Storia Naturale, Sezione di Mineralogia, Università di Firenze, Via La Pira 4, I-50121 Firenze, Italy
²École Polytechnique Fédérale de Lausanne, Laboratoire de Cristallographie, BSP, CH-1015 Lausanne, Switzerland

ABSTRACT

Structural investigations of several minerals belonging to the calaverite group with composition $\text{Au}_{1-x}\text{Ag}_x\text{Te}_2$ ($x = 0.00, 0.02, 0.05, 0.09, 0.19,$ and 0.33) indicate that Ag is randomly distributed on the Au sites. This suppresses the valence fluctuation of Au and, therefore, the structure modulations. The results are compared with the previously published incommensurately modulated structure of calaverite, $\text{Au}_{0.9}\text{Ag}_{0.1}\text{Te}_2$, which is characterized by valence fluctuations of Au reinforced by an ordered distribution of Ag. The (3+1)-dimensional calaverite structure type is able to reproduce both (3+1)D and 3D related structures with the general formula AB_2 ($A = \text{Au}, \text{Ag}, \text{Cu}, \text{Nb}, \text{Ta}; B = \text{Te}$).

Keywords: Calaverite, modulated structure, valence fluctuations, krennerite

INTRODUCTION

Calaverite was first identified by Ghent (1861) and, since its discovery, it has been the subject of numerous studies, in large part because of the difficulties mineralogists encountered in indexing crystalline specimens from different locations. It was later found that the diffraction pattern of calaverite exhibited satellite reflections, which pointed to the presence of an incommensurately modulated structure (Chapuis 2003 and references therein). Calaverite belongs to the group of gold-silver tellurides with the chemical formula $\text{Au}_{1-x}\text{Ag}_x\text{Te}_2$, the most important group of minerals from an economic standpoint in the Au-Ag-Te system. This group comprises calaverite, AuTe_2 (the monoclinic polymorph); krennerite, AuTe_2 (the orthorhombic polymorph); and sylvanite, AuAgTe_4 . Based on the experimental data of Cabri (1965), calaverite, krennerite, and sylvanite contain 0.00 to 2.8 wt%, 3.4 to 6.2 wt%, and 6.7 to 13.2 wt% Ag, respectively. These minerals occur in several epizonal and mesozonal gold and gold-silver telluride deposits including the Golden Mile, Kalgoorlie, Australia (e.g., Clout et al. 1990; Shackleton et al. 2003), Emperor, Fiji (e.g., Ahmad et al. 1987; Pals and Spry 2003), Cripple Creek, Colorado (e.g., Thompson et al. 1985), and Săcărîmb, Romania (Alderton and Fallick 2000) deposits, which are among the largest gold deposits in the world.

From the crystallographic standpoint, calaverite has received much attention in the past century because its morphology was considered to violate Haüy's law of rational indices (Goldschmidt et al. 1931 and references therein). It is surprising that the introduction of diffraction techniques did not solve the puzzle initially. Indeed, it was first Tunell and Ksanda (1936) and then Tunell and Pauling (1952) who were able to solve the average $C2/m$ structure of calaverite. However, they did not propose any interpretation of the so-called "adventive diffraction spots" (now called satellites) observed in the diffraction pattern of calaverite.

Sueno et al. (1979) were the first to identify the additional spots as "wavy displacements" in the structure. These authors found that the satellite positions were at 27.3° from the $+c^*$ axis and 62.7° from the $+a^*$ axis, with a wave vector normal to the $(30\bar{4})$ lattice plane. Nonetheless, Sueno et al. (1979) could not solve the structure with a sinusoidal wave-distribution function for the displacement of the Te atoms in a commensurate enlarged supercell. Later, based on a transmission electron microscopy (TEM) study, Van Tendeloo et al. (1983a) pointed out that the satellite reflections in calaverite were due to an incommensurately displacive modulation superimposed on the average $C2/m$ structure. Using the information gained from the TEM study, Dam et al. (1985) were able to clarify the morphology of calaverite by indexing the crystal faces with four instead of three indices, the extra index applying to $\mathbf{q} = -0.4095\mathbf{a}^* + 0.4492\mathbf{c}^*$. Finally, Schutte and de Boer (1988), using the superspace approach, solved the incommensurately modulated structure of calaverite in the superspace group $C2/m(\alpha 0\gamma)0s$. These authors showed that the modulation consists mainly of displacements of Te atoms and the observed modulations are interpreted in terms of valence fluctuations between Au^+ and Au^{3+} . More recently, Balzuweit et al. (1993) studied the variation of the modulation wave vector in synthetic calaverite as a function of temperature and silver content (up to 3.0 at% of Ag) using X-ray diffraction and morphological techniques.

In the course of research projects dealing with the characterization of tellurium-bearing minerals from museum collections (Bindi and Cipriani 2003a, 2003b, 2004a, 2004b, 2004c, 2004d; Bindi et al. 2004, 2005; Bindi 2008, 2009), we analyzed calaverite samples with variable silver contents. The aim of the present work is to characterize calaverite by single-crystal X-ray diffraction, scanning electron microscopy (SEM), and electron probe microanalysis (EPMA) and to discuss the role of silver in the stabilization of the incommensurately modulated structure in the framework of the superspace concept.

* E-mail: luca.bindi@unifi.it

OCCURRENCE, PHYSICAL AND OPTICAL PROPERTIES

A list of the samples investigated in this study, together with their locations and chemical formulae, is given in Table 1. All the samples came from the mineralogical collection of the Museo di Storia Naturale, Università di Firenze. The calaverite samples have colors ranging from yellow to silver white, show a greenish to yellowish gray streak and exhibit a metallic luster. The crystals are brittle and their fractures are uneven to subconchoidal. Micro-indentation measurements carried out with a VHN load of 100 g give the mean values reported in Table 2.

In plane-polarized incident light, calaverite is white in color, with moderate bireflectance (from white to brownish gray). Under crossed polars, calaverite shows weak anisotropism without internal reflections. Reflectance measurements were performed for all the samples in air by means of a MPM-200 Zeiss microphotometer equipped with a MSP-20 system processor on a Zeiss Axioplan ore microscope. The filament temperature was approximately 3350 K. An interference filter was adjusted to select, in turn, four wavelengths for measurement (471.1, 548.3, 586.6, and 652.3 nm). Readings were taken for the specimen and standard (SiC) under the same focus conditions. The diameter of the circular measuring area was 0.1 mm. Reflectance percentages for R_{min} and R_{max} are given in Table 3. It appears that the reflectivity values decrease with the increase of silver replacing gold.

Chemical composition

Qualitative chemical analysis using energy dispersive spectrometry, performed on the crystal fragments used for the structural study, did not indicate the presence of elements ($Z > 9$) other than Ag, Au, and Te. Quantitative chemical compositions were then determined using wavelength dispersive analysis (WDS) by means of a JEOL JXA-8600 electron microprobe. Concentrations of major and minor elements were determined at an accelerating voltage of 20 kV and a beam current of 40 nA, with 10 s as the counting time. For the WDS analyses, the following lines were used: $AgL\alpha$, $AuM\alpha$, and $TeL\alpha$. The standards employed were

native elements for Ag, Au, and Te. The crystal fragments were found to be homogeneous within the analytical errors. The average chemical compositions (six to eight analyses on each grain) are reported in Table 4. The chemical formulae were calculated on the basis of three atoms.

Single-crystal X-ray diffraction

The diffraction quality of the single crystals was initially checked by means of an Enraf-Nonius CAD4 single crystal diffractometer equipped with a conventional point detector. The crystals were then carefully investigated using an Oxford Diffraction “Xcalibur 3” single-crystal diffractometer (enhanced X-ray source, X-ray radiation $MoK\alpha$, $\lambda = 0.71073 \text{ \AA}$) fitted with a Sapphire 2 CCD detector. A total of 500 frames of data were collected¹ for each crystal at room temperature consisting of 5 sets of omega runs with an exposure time of 30 s per frame and a frame width of 0.75°. Data frames were processed using the CrysAlis software package (Oxford Diffraction 2006) running on the Xcalibur 3 control PC. A relatively high $\sin(\theta)/\lambda$ cut off and a high redundancy were chosen in the recording settings. Unit-cell parameters for the selected crystals are given in Table 5. The modulation wave vectors (Table 6) were obtained by the least-squares refinement of the setting angles of the first-order satellites along with the main reflections. Only first-order satellites could be observed after integration for $Ag_{0.09}$, $Ag_{0.05}$, $Ag_{0.02}$, and $Ag_{0.00}$. No satellites have been detected for the Ag-rich members. Other crystals tested from the different samples (3–4 for each sample) gave similar results both in terms of observed

TABLE 1. List of the calaverite samples studied

Sample	Label	Provenance	Chemical formula
2400/I	Ag _{0.00}	Kotchbulak, Uzbekistan	Au _{0.99} Te _{2.01}
48028/G	Ag _{0.02}	Kalgoorlie, Australia	(Au _{0.97} Ag _{0.02})Te _{2.01}
898/G	Ag _{0.05}	Colorado, U.S.A.	(Au _{0.95} Ag _{0.05})Te _{2.00}
894/G	Ag _{0.09}	Nagyag, Transylvania, Romania	(Au _{0.90} Ag _{0.09})Te _{2.01}
884/G	Ag _{0.19}	Offenbanya, Transylvania, Romania	(Au _{0.83} Ag _{0.19})Te _{1.98}
885/G	Ag _{0.33}	Offenbanya, Transylvania, Romania	(Au _{0.66} Ag _{0.33})Te _{1.99}

TABLE 2. Mean microhardness (kg/mm²) values for the calaverite samples investigated

Sample	Mean value	Range
Ag _{0.00}	169	160–175
Ag _{0.02}	180	172–187
Ag _{0.05}	189	180–194
Ag _{0.09}	194	188–199
Ag _{0.19}	197	192–204
Ag _{0.33}	199	193–207

TABLE 3. R_{min} and R_{max} values (%) for the calaverite samples investigated

Wavelength (nm)	Ag _{0.00}	Ag _{0.02}	Ag _{0.05}	Ag _{0.09}	Ag _{0.19}	Ag _{0.33}
471.1	56.2–61.8	56.0–61.3	55.7–61.0	54.3–60.2	53.0–56.8	50.1–53.8
548.3	61.2–66.3	60.9–65.9	60.3–65.1	59.5–64.2	58.3–63.0	56.2–60.9
586.6	63.2–68.0	63.0–67.5	62.3–67.2	61.5–66.2	60.1–65.4	57.2–62.7
652.3	65.4–69.8	65.1–69.6	64.7–69.3	64.1–68.5	63.1–67.0	60.4–64.7

¹ Deposit item AM-09-025, CIFs. Deposit items are available two ways: For a paper copy contact the Business Office of the Mineralogical Society of America (see inside front cover of recent issue) for price information. For an electronic copy visit the MSA web site at <http://www.minsocam.org>, go to the American Mineralogist Contents, find the table of contents for the specific volume/issue wanted, and then click on the deposit link there.

TABLE 4. Electron microprobe analyses (means and ranges in wt% of elements) and atomic ratios (calculated on the basis of 3 atoms) of the selected calaverite crystals

	Ag _{0.00}	Ranges	Ag _{0.02}	Ranges	Ag _{0.05}	Ranges
Au	42.94	(42.63–43.40)	42.43	(42.09–42.99)	41.70	(41.33–42.07)
Ag	–	(0.00–0.03)	0.48	(0.35–0.60)	1.20	(1.11–1.36)
Te	56.47	(56.00–57.12)	56.94	(56.05–57.58)	56.87	(56.64–57.39)
Total	99.41	(99.13–100.22)	99.85	(99.65–100.44)	99.77	(99.42–100.51)
Au	0.99		0.97		0.95	
Ag	–		0.02		0.05	
Te	2.01		2.01		2.00	
	Ag _{0.09}	Ranges	Ag _{0.19}	Ranges	Ag _{0.33}	Ranges
Au	40.05	(39.66–40.25)	37.63	(37.25–38.03)	31.60	(31.25–32.34)
Ag	2.19	(1.95–2.30)	4.69	(4.50–4.81)	8.40	(8.11–8.60)
Te	57.96	(57.60–58.23)	57.84	(57.44–58.12)	59.90	(59.45–60.23)
Total	100.20	(99.32–100.66)	100.16	(99.17–100.42)	99.90	(99.42–100.01)
Au	0.90		0.83		0.68	
Ag	0.09		0.19		0.33	
Te	2.01		1.98		1.99	

TABLE 5. Unit-cell parameters for the selected calaverite crystals

Sample	<i>a</i> (Å)	<i>b</i> (Å)	<i>c</i> (Å)	β (°)	<i>V</i> (Å ³)
Ag _{0.00}	7.1901(5)	4.4077(3)	5.0701(4)	90.037(2)	160.68(2)
Ag _{0.02}	7.1945(5)	4.4101(3)	5.0790(5)	90.035(2)	161.15(2)
Ag _{0.05}	7.2115(5)	4.4123(2)	5.0912(5)	90.028(2)	162.00(2)
Ag _{0.09}	7.2356(4)	4.4160(3)	5.1112(4)	90.030(3)	163.32(2)
Ag _{0.19}	7.2998(5)	4.4250(3)	5.1563(4)	90.032(3)	166.56(2)
Ag _{0.33}	7.4002(4)	4.4366(2)	5.2416(5)	90.034(2)	172.09(2)

TABLE 6. Modulation wave vectors for the selected calaverite crystals

Sample	Modulation wave vector
Ag _{0.00}	-0.4026(2) a * + 0.4470(2) c *
Ag _{0.02}	-0.4051(2) a * + 0.4479(2) c *
Ag _{0.05}	-0.4071(3) a * + 0.4491(3) c *
Ag _{0.09}	-0.4112(2) a * + 0.4511(2) c *
Ag _{0.19}	—
Ag _{0.33}	—

satellites and modulation wave vectors. In an attempt to detect observable satellites for the Ag-rich members, a second measurement was performed with longer exposure times (400 s). No appreciable time-dependent change in intensities and/or positions of both main and satellite reflections was observed. A similar result was obtained when the same crystals were collected at a temperature ca. 110 K, the low temperature being achieved by means of an Oxford cryostream cooler. Before measurement, the samples were held at the specified temperature for about 180 min. After the cooling experiment, the crystals were re-heated to ca. 300 K, and new data were collected. The obtained unit-cell parameter and modulation wave vectors did not reveal significant variation from the previous ones. Intensity integration and

standard Lorentz-polarization correction were performed with the CrysAlis RED (Oxford Diffraction 2006) software package. The program ABSPACK in CrysAlis RED was applied for the absorption correction. The least-squares program JANA2006 (Petříček et al. 2006) was used for the refinements of all the structures. Neutral scattering curves for Au, Ag, and Te were taken from the *International Tables for X-ray Crystallography* (Ibers and Hamilton 1974). Refinements of the incommensurately modulated structures were performed in the superspace group *C2/m*($\alpha 0\gamma$)0s for Ag_{0.00}, Ag_{0.02}, Ag_{0.05}, and Ag_{0.09} and in the space group *C2/m* for Ag_{0.19} and Ag_{0.33} (no satellites detected). Experimental details of the data collections and refinements are given in Table 7. Fractional atomic coordinates, anisotropic displacement parameters, and selected bond distances are reported in Tables 8–11.

The incommensurately modulated structures of Ag_{0.00}, Ag_{0.02}, Ag_{0.05}, and Ag_{0.09} have been refined according to the following scheme: first, the average structure was refined. Then the first harmonic of positional modulation wave was introduced for both Te and (Au,Ag). The only possible amplitude of the (Au,Ag) positional modulation (Table 8) was equal to 0 within 1 standard deviation for Ag_{0.00} and Ag_{0.02} and within 2 standard deviations for Ag_{0.05} (Table 8). The refinement of the Te positional modulation improved all *R* factors; however, the essential decrease of *R*_{satellite}, from about 15% to about 7%, was reached by applying an additional crenel function (0.5 length along *t*₄ with the center at *t*₄ = 0.25) for Ag_{0.00}, Ag_{0.02}, and Ag_{0.05}. This crenel function results in a small shift of Te from the mirror plane [*y*_{Te} ≈ -0.04 to -0.02 (Table 8)]. The refined contributions of Ag in

TABLE 7. Data and experimental details for the selected calaverite crystals

	Ag _{0.00}	Ag _{0.02}	Ag _{0.05}	Ag _{0.09}	Ag _{0.19}	Ag _{0.33}
Temperature (K)	298	298	298	298	298	298
Cell setting	monoclinic	monoclinic	monoclinic	monoclinic	monoclinic	monoclinic
Superspace group/ Space group	<i>C2/m</i> ($\alpha 0\gamma$)0s	<i>C2/m</i>	<i>C2/m</i>			
Crystal color	yellow	yellow	yellow	yellow	yellow	yellow
Crystal shape	irregular	irregular	irregular	irregular	irregular	irregular
Crystal size (mm)	0.11 × 0.12 × 0.13	0.09 × 0.10 × 0.13	0.08 × 0.09 × 0.11	0.10 × 0.10 × 0.12	0.07 × 0.09 × 0.10	0.07 × 0.11 × 0.12
Diffractometer	Oxford	Oxford	Oxford	Oxford	Oxford	Oxford
Diffraction	Diffraction	Diffraction	Diffraction	Diffraction	Diffraction	Diffraction
Xcalibur 3	Xcalibur 3	Xcalibur 3	Xcalibur 3	Xcalibur 3	Xcalibur 3	Xcalibur 3
Radiation	MoK-L _{2,3} (0.71073 Å)					
Monochromator	graphite	graphite	graphite	graphite	graphite	graphite
Scan mode	φ/ω	φ/ω	φ/ω	φ/ω	φ/ω	φ/ω
Detector to sample distance (cm)	5	5	5	5	5	5
Measuring time (s)	30	30	30	30	30	30
Theta range (°)	1–45	1–45	1–45	1–45	1–45	1–45
Range of <i>h,k,l,m</i>	-14 ≤ <i>h</i> ≤ 14 -8 ≤ <i>k</i> ≤ 8 -10 ≤ <i>l</i> ≤ 10 -1 ≤ <i>m</i> ≤ 1	-14 ≤ <i>h</i> ≤ 14 -8 ≤ <i>k</i> ≤ 8 -10 ≤ <i>l</i> ≤ 10 -1 ≤ <i>m</i> ≤ 1	-14 ≤ <i>h</i> ≤ 14 -8 ≤ <i>k</i> ≤ 8 -10 ≤ <i>l</i> ≤ 10 -1 ≤ <i>m</i> ≤ 1	-14 ≤ <i>h</i> ≤ 14 -8 ≤ <i>k</i> ≤ 8 -10 ≤ <i>l</i> ≤ 10 -1 ≤ <i>m</i> ≤ 1	-14 ≤ <i>h</i> ≤ 14 -8 ≤ <i>k</i> ≤ 8 -10 ≤ <i>l</i> ≤ 10 -1 ≤ <i>m</i> ≤ 1	-14 ≤ <i>h</i> ≤ 14 -8 ≤ <i>k</i> ≤ 8 -10 ≤ <i>l</i> ≤ 10 -1 ≤ <i>m</i> ≤ 1
No. of measured refl.	5289	5312	5302	5344	5401	5398
No. of unique refl.	788	756	751	746	738	727
No. of observed refl.	698	678	677	681	684	651
Criterion for obs.	<i>I</i> > 3 σ (<i>I</i>)					
<i>R</i> _{int}	0.057	0.105	0.037	0.064	0.039	0.056
Refinement coefficient	<i>F</i>	<i>F</i>	<i>F</i>	<i>F</i>	<i>F</i>	<i>F</i>
No. of refined parameters	34	34	35	35	13	13
Weighting scheme	$w = 1 / [\sigma^2(F)^2 + (0.0001(F)^2)]$					
<i>R</i> , <i>wR</i> (all reflections)	0.0479, 0.0579	0.0383, 0.0385	0.0326, 0.0327	0.0426, 0.0551	0.0230, 0.0235	0.0189, 0.0197
<i>R</i> , <i>wR</i> (main reflections)	0.0470, 0.0544	0.0365, 0.0366	0.0313, 0.0314	0.0421, 0.0538	0.0230, 0.0235	0.0189, 0.0197
<i>R</i> , <i>wR</i> (satellites)	0.0751, 0.0929	0.0764, 0.0767	0.0676, 0.0677	0.0931, 0.1163	—	—
Diff. Fourier (e ⁻ /Å ³)	[-0.38, 0.38]	[-0.05, 0.05]	[-0.01, 0.01]	[-0.35, 0.28]	[-0.27, 0.31]	[-0.18, 0.22]

TABLE 8. Final values of coordinates and Fourier amplitudes of the displacive modulation functions and equivalent isotropic displacement parameters (\AA^2)

	Occupancy	Wave	x	y	z	U_{iso}
Ag_{0.00}						
Au	1.000Au	s,1	0	0	0	0.02352(9)
		c,1	0	0	0	
Te	1.000Te	s,1	0.6917(12)	-0.024(4)	0.295(3)	0.035(2)
		c,1	-0.0051(19)	0.031(5)	-0.012(4)	
			0.0051(6)	-0.0313(6)	0.0105(11)	
Ag_{0.02}						
Au	0.98Au + 0.02Ag	s,1	0	0	0	0.02390(6)
		c,1	0	0	0	
Te	1.000Te	s,1	0.6889(12)	-0.035(4)	0.290(2)	0.029(3)
		c,1	-0.0008(19)	0.043(6)	-0.004(4)	
			0.0050(8)	-0.0283(5)	0.0099(17)	
Ag_{0.05}						
Au	0.948(3)Au + 0.052Ag	s,1	0	0	0	0.02342(5)
		c,1	0	-0.0012(6)	0	
Te	1.000Te	s,1	0.6886(9)	-0.0448(3)	0.2894(13)	0.0303(11)
		c,1	-0.0009(13)	0.0543	-0.003(2)	
			0.0053(6)	-0.0293(4)	0.0099(10)	
Ag_{0.09}						
Au	0.908(8)Au + 0.092Ag	s,1	0	0	0	0.02235(16)
		c,1	0	0.0199(7)	0	
Te	1.000Te	s,1	0.68788(8)	0	0.28710(11)	0.03501(15)
		c,1	0	-0.0044(10)	0	
			0	-0.0076(8)	0	
Ag_{0.19}						
Au	0.888(3)Au + 0.112Ag		0	0	0	0.02288(6)
Te	1.000Te		0.68692(5)	0	0.28722(7)	0.0324(1)
Ag_{0.33}						
Au	0.782(3)Au + 0.218Ag		0	0	0	0.02274(5)
Te	1.000Te		0.68552(3)	0	0.28681(5)	0.02951(7)

Note: The waves are sorted by the terms (s for sinus, c for cosinus) and m.

the (Au,Ag) position confirm the chemical analysis for Ag_{0.05} and Ag_{0.09}. For Ag_{0.02}, the Ag value was fixed at 0.02 because of its uncertainty, which was equal to the value of the Ag contribution, i.e., 0.02(2). Refinement of the ordered distribution of Ag on the Au/Ag position is not justified following the absence of second-order satellites, which should appear as a result of the occupation modulations (Schutte and de Boer 1988). Refinement of the ADP modulations (Table 9) improved all the *R* factors.

The refinement of Ag_{0.19} and Ag_{0.33} did not present any problem. Nevertheless, in both cases the refined occupancies for silver in the (Au,Ag) positions yielded lower Ag contents in comparison to those obtained by electron microprobe analyses [refined values: 0.112(3)Ag and 0.218(3)Ag for Ag_{0.19} and Ag_{0.33}, respectively].

DISCUSSION

Crystal chemistry and structure modulations

The crystal structure of calaverite (Pertlik 1984a; Schutte and de Boer 1988; Reithmayer et al. 1993) is represented in Figure 1. It is based on a distorted hexagonal closed-packed array of Te²⁻ anions with Au (and Ag) cations occupying the octahedral sites. AuTe₆ octahedra form sheets parallel to (001) that are linked by Te-Te bonds.

The refinement of the site-occupancy factor of the (Au,Ag) position in all the investigated calaverite crystals indicates that Ag randomly substitutes for Au in the octahedral site. A strong differentiation of the (Au,Ag)-Te distances is observed for all

the samples independently of the compositions. Two distances are essentially shorter than the other four (Tables 10 and 11; Fig. 2, left), so that the coordination number (CN) of (Au,Ag) can be generally considered as CN = 2 + 4. The mean bond distances range from 2.87 Å in Ag_{0.00} to 2.93 Å in Ag_{0.33}. This increase is not uniform and reflects mainly the two shortest distances, which vary from 2.67 to 2.77 Å, while the mean value of the other four distances changes by only 0.04 Å, from 2.97 to 3.01 Å, with increasing the amounts of Ag (Fig. 2, left). The two short distances remain nearly constant throughout the modulated structures; their variation along the *t*-axis is <2 standard deviations (Table 10, Fig. 2, left). By contrast, the four long distances vary along the *t*-axis, depending on the Ag contribution in the (Au,Ag) position (Fig. 2, left). For the lower Ag contents (i.e., Ag_{0.00}, Ag_{0.02}, and Ag_{0.05}), this variation points to an additional differentiation of

CN of (Au,Ag): two long distances are essentially shorter and two others are essentially longer than their mean value (Fig. 2, left). Moreover, only two long distances and CN = 2 + 2 can be considered in two symmetrically related ranges along the *t*-axis, $-0.05 < t < 0.05$ and $0.45 < t < 0.55$ (gray areas in Fig. 2, left); two additional distances are >3.1 Å. In the remaining ranges, $0.05 < t < 0.45$ and $0.55 < t < 0.95$, the coordination number of (Au,Ag) can be considered as CN = 2 + 4 for Ag_{0.00}, Ag_{0.02}, and Ag_{0.05}. With increasing Ag content (i.e., Ag_{0.09}, Ag_{0.19}, and Ag_{0.33}), the coordination number of (Au,Ag) tends to converge to CN = 2 + 4 (Fig. 2, left). According to Schutte and de Boer (1988), the displacive modulation of the atoms resulting in the differentiation of CN is associated with a valence fluctuation of Au⁺ and Au³⁺; in addition, the occupation modulation of the (Au,Ag) position (ordered distribution of Ag) strengthens this valence fluctuation and the CN differentiation (dashed line graphs in Fig. 2). Our results confirm and complete their conclusion. Indeed, the differentiation of the CN is associated with a significant differentiation of the bond valence sum calculated for Au in Ag_{0.00} (Fig. 2, top right). This differentiation of the bond valence sum disappears consistently with increased randomness of the Ag distribution, so that starting from Ag_{0.19} the structure loses its modulation character. Hence, one can conclude that randomly distributed Ag suppresses the valence fluctuation of Au⁺ and Au³⁺, whereas an ordered distribution reinforces it.

A portion of the incommensurately modulated structures of Ag_{0.00} and Ag_{0.09} (present work) is shown in Figure 3, in comparison with the corresponding portion of the incommensurately

TABLE 9. Final values of the anisotropic displacement parameters (\AA^2) and Fourier amplitudes of the displacive modulation functions

Wave	U_{11}	U_{22}	U_{33}	U_{12}	U_{13}	U_{23}
Ag_{0.00}						
Au	0.02294(15)	0.02287(15)	0.02476(15)	0	0.00011(8)	0
s,1	0	0	0	0	0	0
c,1	0	0	0	-0.0037(4)	0	0.0011(3)
Te	0.020(3)	0.058(4)	0.028(3)	0.014(3)	0.0040(18)	0.022(3)
s,1	0.011(4)	-0.007(6)	0.001(5)	-0.015(3)	-0.009(3)	-0.021(4)
c,1	0.0002(10)	-0.007(2)	-0.0023(12)	0.0006(9)	-0.0021(10)	0.0005(12)
Ag_{0.02}						
Au	0.02302(10)	0.02290(11)	0.02576(10)	0	0.00012(6)	0
s,1	0	0	0	0	0	0
c,1	0	0	0	-0.0031(4)	0	0.0023(4)
Te	0.024(4)	0.040(7)	0.024(3)	0.0053(16)	-0.003(2)	0.011(2)
s,1	0.005(6)	0.006(10)	0.010(4)	-0.007(2)	0.002(3)	-0.008(3)
c,1	0.0001(7)	-0.004(2)	-0.0007(6)	0.0015(13)	-0.0010(4)	0.0011(17)
Ag_{0.05}						
Au	0.02283(9)	0.02252(9)	0.02492(9)	0	0.00010(5)	0
s,1	0	0	0	0	0	0
c,1	0	0	0	-0.0035(4)	0	0.0021(4)
Te	0.036(2)	0.0296(19)	0.0256(16)	0.0070(13)	-0.0049(12)	0.0106(10)
s,1	-0.012(3)	0.007(3)	0.006(3)	-0.0074(13)	0.0047(18)	-0.0065(11)
c,1	-0.0017(9)	-0.0021(13)	-0.0005(5)	0.0006(7)	-0.0006(4)	0.0008(8)
Ag_{0.09}						
Au	0.02285(14)	0.0186(4)	0.02564(16)	0	0.00025(9)	0
s,1	0	0	0	0	0	0
c,1	0	0	0	0.0010(8)	0	0.0071(7)
Te	0.0289(2)	0.0444(3)	0.0318(2)	0	-0.00067(17)	0
s,1	0	0	0	-0.0042(12)	0	-0.0075(11)
c,1	0	0	0	-0.0036(15)	0	0.0065(13)
Ag_{0.19}						
Au	0.02285(9)	0.02182(9)	0.02398(9)	0	0.00017(6)	0
Te	0.0298(2)	0.0370(2)	0.0304(2)	0	-0.0009(1)	0
Ag_{0.33}						
Au	0.02293(7)	0.02216(8)	0.02312(7)	0	0.00016(5)	0
Te	0.0298(1)	0.0293(1)	0.0294(1)	0	-0.00086(8)	0

TABLE 10. The interatomic distances (\AA) and angles ($^\circ$) in the modulated structures of Ag_{0.00}, Ag_{0.02}, Ag_{0.05}, and Ag_{0.09}

	Ag _{0.00}			Ag _{0.02}			Ag _{0.05}			Ag _{0.09}		
	average	minimal	maximal	average	minimal	maximal	average	minimal	maximal	average	minimal	maximal
Au-Te ^a	2.675(15)	2.671(18)	2.684(12)	2.678(15)	2.673(18)	2.693(12)	2.688(9)	2.682(11)	2.703(8)	2.694(6)	2.6939(6)	2.6945(7)
Au-Te ^b	2.99(2)	2.87(2)	3.219(16)	3.00(2)	2.89(2)	3.228(17)	3.010(7)	2.890(7)	3.267(5)	2.980(3)	2.904(4)	3.056(4)
Au-Te ^c	2.95(2)	2.870(15)	3.00(2)	2.95(2)	2.826(17)	3.00(3)	2.943(7)	2.796(6)	3.015(7)	2.979(3)	2.904(4)	3.056(4)
Au-Te ^d	2.675(15)	2.671(18)	2.684(12)	2.679(15)	2.673(18)	2.693(12)	2.688(9)	2.682(11)	2.703(8)	2.694(6)	2.6939(6)	2.6945(7)
Au-Te ^e	2.98(2)	2.87(2)	3.219(16)	3.00(2)	2.89(2)	3.228(17)	3.007(7)	2.890(7)	3.267(5)	2.979(3)	2.904(4)	3.056(4)
Au-Te ^f	2.96(2)	2.870(15)	3.00(2)	2.95(2)	2.826(17)	3.00(3)	2.945(7)	2.796(6)	3.015(7)	2.980(3)	2.904(4)	3.056(4)
Te ^a -Au-Te ^b	97.9(6)	96.0(7)	98.7(6)	97.5(6)	95.8(7)	98.2(6)	97.4(3)	95.8(3)	98.2(3)	96.54(8)	95.47(8)	97.60(8)
Te ^a -Au-Te ^c	96.4(6)	96.0(5)	97.1(7)	96.5(6)	96.1(6)	97.6(5)	96.6(3)	96.0(3)	98.1(2)	96.55(8)	95.47(8)	97.60(8)
Te ^a -Au-Te ^d	169.7(7)	169.7(7)	169.7(7)	168.4(8)	168.4(8)	168.4(8)	166.32(7)	166.32(7)	166.32(7)	178.56(15)	177.72(19)	180
Te ^a -Au-Te ^e	83.8(6)	83.4(5)	83.9(6)	83.4(6)	82.2(5)	84.2(7)	83.3(3)	81.6(3)	84.4(3)	83.43(7)	82.66(7)	84.21(7)
Te ^a -Au-Te ^f	81.7(6)	81.4(6)	82.6(5)	82.2(6)	81.8(6)	83.3(5)	82.3(3)	81.7(3)	83.8(2)	83.44(7)	82.66(7)	84.21(7)
Te ^b -Au-Te ^d	83.8(6)	83.4(7)	83.9(6)	83.4(7)	82.2(7)	84.2(6)	83.3(2)	81.6(3)	84.4(2)	83.44(8)	82.66(8)	84.21(8)
Te ^b -Au-Te ^e	84.2(6)	83.4(6)	84.7(7)	84.1(7)	82.2(6)	85.1(7)	84.1(2)	81.7(2)	85.5(2)	84.37(9)	81.93(11)	86.86(13)
Te ^b -Au-Te ^f	178.8(6)	177.9(6)	179.9(5)	178.7(6)	176.7(6)	179.9(5)	178.5(2)	176.0(2)	179.9(3)	178.44(9)	177.53(12)	180
Te ^c -Au-Te ^d	81.7(6)	81.4(6)	82.6(7)	82.2(7)	81.8(6)	83.3(7)	82.3(2)	81.7(2)	83.8(3)	83.43(8)	82.66(8)	84.21(8)
Te ^c -Au-Te ^e	178.8(6)	177.9(6)	179.9(5)	178.7(6)	176.7(6)	179.9(5)	178.5(2)	176.0(2)	179.9(3)	178.44(9)	177.53(12)	180
Te ^c -Au-Te ^f	82.8(6)	81.1(7)	85.6(6)	83.3(7)	81.7(7)	86.1(6)	83.4(2)	81.6(2)	86.7(2)	84.37(9)	81.93(11)	86.86(13)
Te ^d -Au-Te ^e	97.9(6)	96.0(7)	98.7(6)	97.5(6)	95.8(7)	98.2(6)	97.5(3)	95.8(3)	98.2(3)	96.55(8)	95.47(8)	97.60(8)
Te ^d -Au-Te ^f	96.4(6)	96.0(5)	97.1(7)	96.5(6)	96.1(6)	97.6(5)	96.6(3)	96.0(3)	98.1(2)	96.54(8)	95.47(8)	97.60(8)
Te ^e -Au-Te ^f	95.8(6)	92.6(6)	97.3(6)	95.8(6)	93.3(6)	97.3(6)	95.7(2)	93.1(2)	97.4(2)	95.63(8)	95.60(8)	95.66(8)

Note: Symmetry codes: (a) $x - 1, y, z$; (b) $x - 1/2, y - 1/2, z$; (c) $x - 1/2, y + 1/2, z$; (d) $-x + 1, y, -z$; (e) $-x + 1/2, y - 1/2, -z$; (f) $-x + 1/2, y + 1/2, -z$.

TABLE 11. Selected bond distances and angles for the average structures of Ag_{0.19} and Ag_{0.33}

	Ag _{0.19}	Ag _{0.33}
Au-Te ($\times 2$)	2.7240(4)	2.7713(3)
Au-Te ($\times 4$)	2.9913(3)	3.0105(2)
mean	2.902	2.931
Te-Au-Te ($\times 4$)	180.00	180.00
Te-Au-Te ($\times 4$)	96.51(1)	96.43(1)
Te-Au-Te ($\times 4$)	83.49(1)	83.57(1)
Te-Au-Te ($\times 2$)	84.60(1)	85.07(1)
Te-Au-Te ($\times 2$)	95.40(1)	94.93(1)
Te-Te	3.2490(4)	3.2900(3)
Te-Te-Te	85.84(2)	84.79(2)

modulated structure of Ag_{0.1} reconstructed using the data of Schutte and de Boer (1988). Distances only shorter than 3.1 \AA are shown in this figure. In Ag_{0.00}, the square coordination of Au (Fig. 3, top) with CN = 2 + 2 and distances 2.67 $\text{\AA} \times 2$ and ~2.88 $\text{\AA} \times 2$ (gray region in Fig. 2, left-top) is associated with the lower valence fluctuation of Au (gray region in Fig. 2, right-top). In Ag_{0.09}, the random distribution of Ag on the (Au,Ag) position leads to a stabilization of the octahedral coordination (CN = 2 + 4) for all the (Au,Ag) atoms (Fig. 3, middle) and the absence of the valence fluctuation of Au (Fig. 2, middle-right). This octahedron

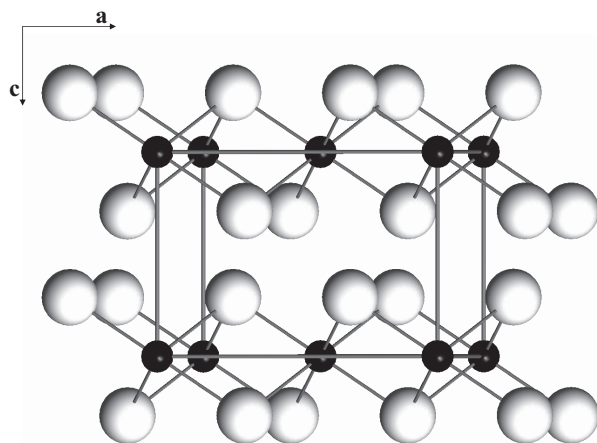


FIGURE 1. The crystal structure of calaverite. Black and white spheres refer to the Au and Te atoms, respectively. The unit cell and the orientation of the structure are outlined.

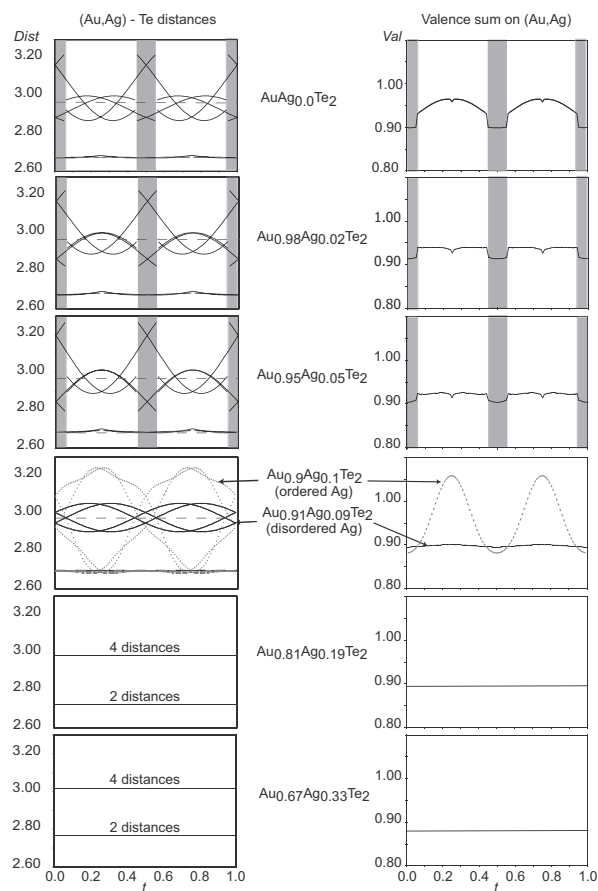


FIGURE 2. Variation of the (Au,Ag)-Te distances (left column) and the bond valence sums on (Au,Ag) (right column) as functions of t . Solid lines correspond to the present work; dashed graphs have been reconstructed using data published by Schutte and de Boer (1988). The gray fields indicate regions with $CN = 2 + 2$.

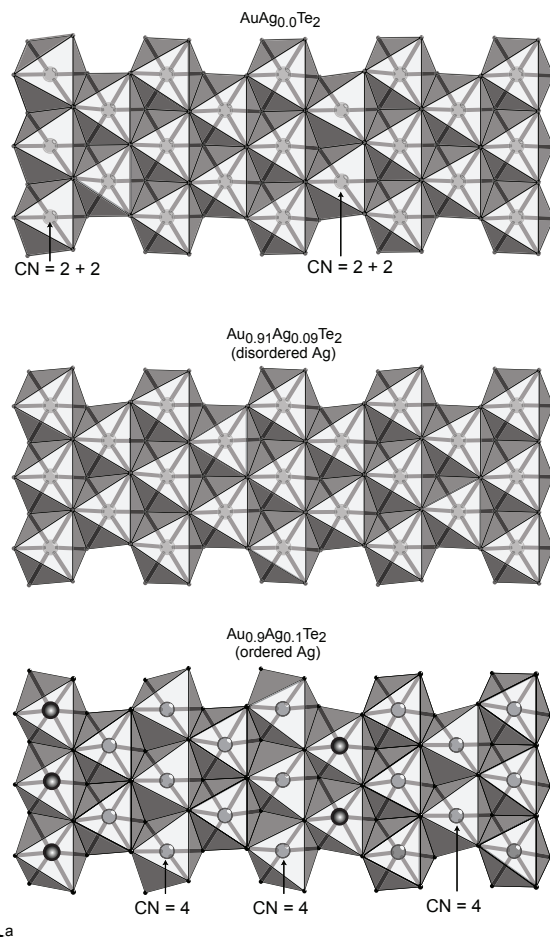


FIGURE 3. [001] projection of a portion of the $Ag_{0.00}$ and $Ag_{0.09}$ incommensurately modulated structures (present work) in comparison with the corresponding part of the $Ag_{0.1}$ structure (Schutte and de Boer 1988). The thick gray lines indicate the (Au,Ag)-Te distances, which are shorter than 3.1 Å. The darker circles represent the (Au,Ag) positions that mainly incorporate Ag.

is also characteristic of the (Au,Ag) positions that mainly incorporate Ag in $Ag_{0.1}$ (darker circles in Fig. 3, bottom). The Ag-free (Au,Ag) positions keep the square coordination (Fig. 3, bottom), and a higher bond valence sum (dashed lines in Fig. 2).

Our investigation of the natural minerals in the series $Au_{1-x}Ag_xTe_2$ completes other studies on calaverite (Pertlik 1984a; Schutte and Boer 1988; Van Tendeloo et al. 1983a; Reithmayer et al. 1993), sylvanite (Van Tendeloo et al. 1983b; Pertlik 1984c), and krennerite (Van Tendeloo et al. 1984; Pertlik 1984b). All these examples taken together show that different degrees of valence fluctuations on the Au-position are possible and, further, these fluctuations can induce the structure modulation.

Variation of the unit-cell parameters and the modulation wave vector

As shown in Figure 4, the incorporation of Ag on the octahedral site causes an anisotropic expansion of the unit cell. Both the a and c parameters (Figs. 4a and 4c) increase linearly,

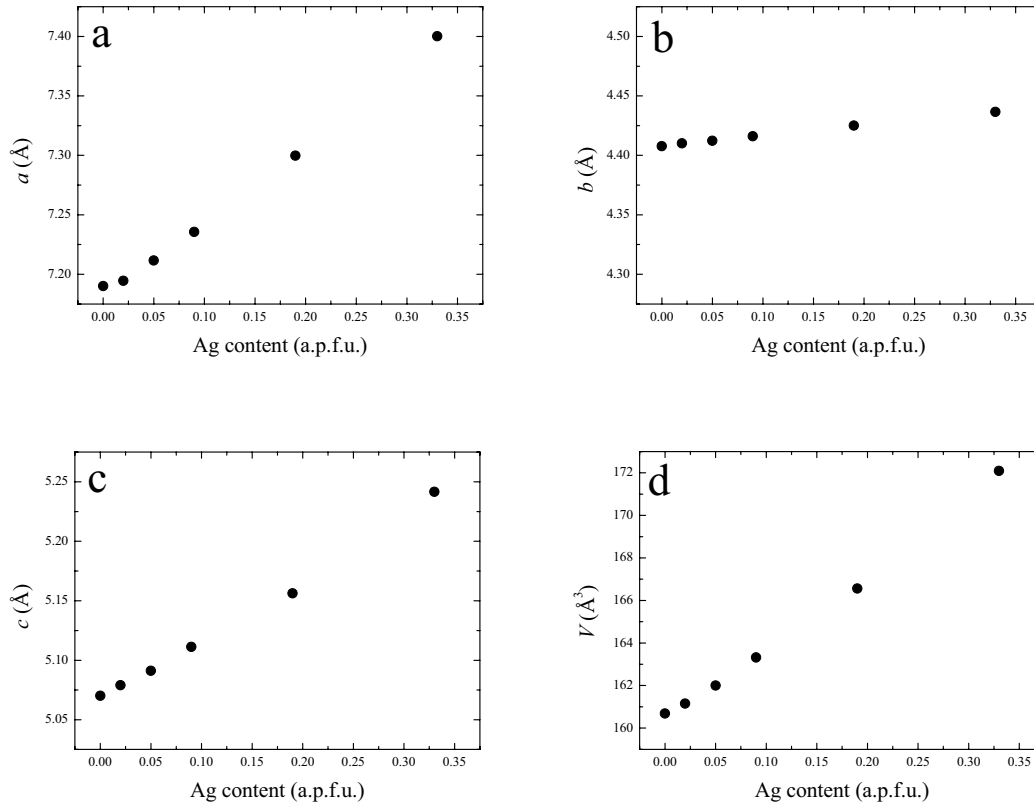


FIGURE 4. Variation of the unit-cell parameters as a function of the Ag content (apfu).

whereas the b parameter remains essentially unchanged (Fig. 4b). No clear trend can be observed for the β angle, which does not appear to be related to the Ag content (Table 5). The marked increase of the a and c parameters as a function of Ag content is mainly related to the pronounced lengthening of the two shortest octahedral distances.

Figure 5 illustrates the variation of the coefficients α and γ of the modulation vector as a function of the Ag content. We observe a constant linear decrease of α and a linear increase of γ with increasing the Ag content. The observed variation of the modulation wave vector indicates that for the samples of calaverite studied here no characteristic phase with a specific \mathbf{q} is observed. Furthermore, the variations in the modulation wave vector (Table 5) are larger than those observed by Balzuweit et al. (1993) for synthetic Ag-bearing calaverites.

The calaverite (3+1)D structure-type family

It is remarkable that calaverite, krennerite, sylvanite, and related compounds can be described within a unique (3+1)D structure-type, similar to another large group of related compounds jointly described within the scheelite (3+1)D structure-type (Arakcheeva and Chapuis 2008). This “calaverite (3+1)D structure type” is characterized by: (1) the (3+1)-dimensional superspace group $C2/m(\alpha 0 \gamma)0s$ with the vector $\mathbf{q} = \alpha \mathbf{a}^* + \gamma \mathbf{c}^*$; (2) unit-cell parameters $a \approx 7.3 \text{ \AA}$, $b \approx 4.3 \text{ \AA}$, $c \approx 5.1 \text{ \AA}$, and $\beta \approx 90^\circ$; and (3) two Wyckoff positions, A (Au, Ag) $-2a: (000)$ and B (Te) $4i: (x0z)$. The coefficients of the \mathbf{q} vector and modulation

functions of both A and B (both positional and occupational) as well as the variable coordinates of the B position are independent variables. Moreover, the incommensurately modulated structure of calaverite (Schutte and de Boer 1988) can be considered as the parent structure for the starting model of the structure refinements (as has been done in the present work), or for the generation of some related structures. For example, the structure of sylvanite can be derived from calaverite with the rational coefficients of $\mathbf{q} = \frac{1}{2}\mathbf{a}^* + 0\mathbf{c}^*$ and an occupation function of A position defined by Ag in the symmetrically related intervals $-0.125 < t < 0.125$ and $0.375 < t < 0.625$ and by Au in the symmetrically related intervals $0.125 < t < 0.375$ and $0.625 < t < 0.875$. The mineral kostovite (CuAuTe_4 ; Van Tendeloo and Amelinckx 1986) is isostructural with sylvanite and can also be included in the calaverite (3+1)D family. The structure of krennerite, $\text{Ag}_{0.2}\text{Au}_{0.8}\text{Te}_2$, can be described as calaverite with ordered twin m -mirror planes leading to orthorhombic symmetry (Van Tendeloo et al. 1984). Some synthetic compounds can also be described in the calaverite (3+1)D structure type. For example, the crystal structures of NbTe_2 , TaTe_2 (Brown 1966), and VTe_2 (Bronsema et al. 1984) correspond to this structure type as commensurately modulated structures with $\mathbf{q} = \frac{1}{3}\mathbf{a}^* + \frac{1}{3}\mathbf{c}^*$.

CONCLUDING REMARKS

The present study of various calaverite samples with the chemical compositions $\text{Au}_{1-x}\text{Ag}_x\text{Te}_2$, $0 \leq x \leq 0.33$, extends the study of Schutte and de Boer (1988) and sheds new light on

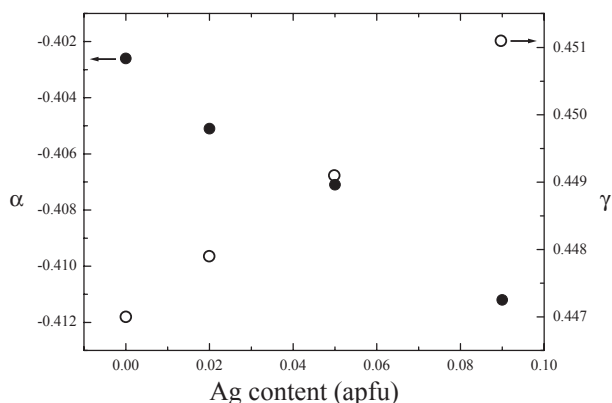


FIGURE 5. Variation of the module α and γ of the modulation vector as a function of the Ag content (apfu).

the origin of the structural modulations observed in this family of compounds. Silver atoms present two types of distribution on the Au sites, either randomly distributed or ordered. The original study of Schutte and de Boer (1988) was concerned with an ordered distribution of Ag, which induces very strong valence fluctuations of Au in the structure. The present study demonstrates another aspect of the $\text{Au}_{1-x}\text{Ag}_x\text{Te}_2$ compounds, specifically those with random distributions of Ag on the Au position. By combining the results of both studies, we contend that the valence fluctuation of Au produces the structure modulation in AuTe_2 . Moreover, the ordered distribution of silver reinforces the valence fluctuation of Au. A random distribution of Ag suppresses the valence fluctuation of Au and, therefore, their structural modulations. Apparently, natural samples can be found with the same composition but with both types of Ag ordering, which is not surprising considering the various growth conditions of the minerals.

Another interesting aspect of the $\text{Au}_{1-x}\text{Ag}_x\text{Te}_2$ series is related to the (3+1)D superspace embedding of the calaverite structure type. We have shown that the same model, independently of their 3D structures and periodicities, can describe all the samples with the same general formula. This formalism opens new perspectives, not only for a uniform description of this family of minerals, but also for other synthetic compounds related to the calaverite structure.

ACKNOWLEDGMENTS

The paper benefited by the official reviews made by P. Spry and an anonymous reviewer. Associate Editor H. Xu is thanked for his efficient handling of the manuscript. This work was funded by M.I.U.R., P.R.I.N. 2007, project "Complexity in minerals: modulation, phase transition, structural disorder" issued to Silvio Menchetti. The support provided by the Swiss National Science Foundation (grant 20-113605) is gratefully acknowledged.

REFERENCES CITED

Ahmad, M., Solomon, M., and Walsh, J.L. (1987) Mineralogical and geochemical studies of the Emperor gold telluride deposit, Fiji. *Economic Geology*, 82, 345–370.

Alderton, D.H.M. and Fallick, A.E. (2000) The nature and genesis of gold-silver-tellurium mineralization in the Metaliferi Mountains of western Romania. *Economic Geology*, 95, 495–516.

Arakcheeva, A. and Chapuis, G. (2008) Capabilities and limitations of a (3 + d)-dimensional incommensurately modulated structure as a model for the

derivation of an extended family of compounds: example of the scheelite-like structures. *Acta Crystallographica*, B64, 12–25.

Balzuweit, K., Hovestad, A., Meeke, H., and de Boer, J.L. (1993) The temperature and composition dependence of the modulation wave vector of incommensurate calaverite. *Journal of Crystal Growth*, 131, 518–532.

Bindi, L. (2008) Commensurate-incommensurate phase transition in muthmannite, AuAgTe_2 : First evidence of a modulated structure at low-temperature. *Philosophical Magazine Letters*, 88, 533–541.

——— (2009) Thermal expansion behavior of empressite, AgTe : A structural study by means of in situ high-temperature single-crystal X-ray diffraction. *Journal of Alloys and Compounds*, 473, 262–264, DOI: 10.1016/j.jallcom.2008.05.043.

Bindi, L. and Cipriani, C. (2003a) Plumbian baksanite from the Tyrny'auz W-Mo deposit, Baksan River valley, northern Caucasus, Russian Federation. *Canadian Mineralogist*, 41, 1475–1479.

——— (2003b) Crystal structure refinement of winstanleyite, TiTe_3O_8 , from the Grand Central Mine, Tombstone, Arizona. *Canadian Mineralogist*, 41, 1469–1473.

——— (2004a) Museumite, $\text{Pb}_5\text{AuSbTe}_2\text{S}_{12}$, a new mineral from the gold-telluride deposit of Sacarimb, Metaliferi Mountains, western Romania. *European Journal of Mineralogy*, 16, 835–838.

——— (2004b) Ordered distribution of Au and Ag in the crystal structure of muthmannite, AuAgTe_2 , a rare telluride from Sacarimb, western Romania. *American Mineralogist*, 89, 1505–1509.

——— (2004c) The crystal structure of skippenite, $\text{Bi}_2\text{Se}_2\text{Te}$, from the Kochkar deposit, southern Urals, Russian Federation. *Canadian Mineralogist*, 42, 835–840.

——— (2004d) Mazzettiite, $\text{Ag}_2\text{HgPbSbTe}_5$, a new mineral for the Findley Gulch, Saguache County, Colorado. *Canadian Mineralogist*, 42, 1739–1743.

Bindi, L., Spry, P.G., and Cipriani, C. (2004) Empressite, AgTe , from the Empress-Josephine Mine, Colorado, U.S.A.: Composition, physical properties and determination of the crystal structure. *American Mineralogist*, 89, 1043–1047.

Bindi, L., Rossell Abrodos, M., Van Tendeloo, G., Spry, P.G., and Cipriani, C. (2005) Inferred phase relations in part of the system Au-Ag-Te: an integrated analytical study of gold ore from the Golden Mile, Kalgoorlie, Australia. *Mineralogy and Petrology*, 83, 283–293.

Bronsema, K.D., Bus, G.W., and Wieggers, G.A. (1984) The crystal structure of vanadium ditelluride, $\text{V}_{1+x}\text{Te}_2$. *Journal of Solid State Chemistry*, 53, 415–421.

Brown, B.E. (1966) The crystal structures of NbTe_2 and TaTe_2 . *Acta Crystallographica*, B20, 264.

Cabri, L.J.P. (1965) Phase relations in the Au-Ag-Te system and their mineralogical significance. *Economic Geology*, 60, 1569–1606.

Chapuis, G. (2003) Crystallographic excursion in superspace. *Crystal Engineering*, 6, 187–195.

Clout, J.M.F., Cleghorn, J.H., and Eaton, P.C. (1990) Geology of the Kalgoorlie gold field. In F.E. Hughes, Ed., *Geology of the Mineral Deposits of Australia and Papua New Guinea*, p. 411–431. Australian Institute of Mineral Metallurgy, Melbourne.

Dam, B., Janner, A., and Donnay, J.D.H. (1985) Incommensurate morphology of calaverite (AuTe_2) crystals. *Physical Review Letters*, 55, 2301–2304.

Ghent, F.A. (1861) Calaverite. *American Journal of Science*, 45, 314–317.

Goldschmidt, V., Palache, C., and Peacock, M. (1931) Über calaverit. *Neues Jahrbuch für Mineralogie*, 63, 1–58.

Ibers, J.A. and Hamilton, W.C., Eds. (1974) *International Tables for X-ray Crystallography*, IV, 366 p. Kynock, Dordrecht.

Oxford Diffraction (2006) CrysAlis RED (Version 1.171.31.2) and ABSPACK in CrysAlis RED. Oxford Diffraction Ltd, Abingdon, Oxfordshire.

Pals, D.W. and Spry, P.G. (2003) Telluride mineralogy of the low-sulfidation epithermal Emperor gold deposit, Vatukoula, Fiji. *Mineralogy and Petrology*, 79, 285–300.

Pertlik, F. (1984a) Kristallchemie natürlicher Telluride III: Die Kristallstruktur des Minerals Calaverit, AuTe_2 . *Zeitschrift für Kristallographie*, 169, 227–236.

——— (1984b) Crystal chemistry of natural tellurides II: redetermination of the crystal structure of krennerite, $(\text{Au}_{1-x}\text{Ag}_x)\text{Te}_2$ with $x \sim 0.2$. *Tschermaks Mineralogische und Petrographische Mitteilungen*, 33, 253–262.

——— (1984c) Kristallchemie natürlicher Telluride I: Verfeinerung der Kristallstruktur des Sylvanits, AuAgTe_4 . *Tschermaks Mineralogische und Petrographische Mitteilungen*, 33, 203–212.

Petříček, V., Dušek, M., and Palatinus, L. (2006) JANA2006, a crystallographic computing system. Institute of Physics, Academy of Sciences of the Czech Republic, Prague.

Reithmayer, K., Steurer, W., Schulz, H., and de Boer, J.L. (1993) High-pressure single-crystal study on calaverite, AuTe_2 . *Acta Crystallographica*, B49, 6–11.

Schutte, W.J. and de Boer, J.L. (1988) Valence fluctuations in the incommensurately modulated structure of calaverite AuTe_2 . *Acta Crystallographica*, B44, 486–494.

Shackleton, J.M., Spry, P.G., and Bateman, R. (2003) Telluride mineralogy of the Golden Mile deposit, Western Australia. *Canadian Mineralogist*, 41, 1503–1524.

- Sueno, S., Kimata, M., and Ohmasa, M. (1979) Modulated Structures 1979. In J.M. Cowley, J.B. Cohen, M.B. Salamon, and J. Wuench, Eds., AIP Conference Proceedings, 53, p. 333. American Institute of Physics, New York.
- Thompson, T.B., Trippel, A.D., and Dwelley, P.C. (1985) Mineralized veins and breccias of the Cripple Creek district, Colorado. *Economic Geology*, 80, 1669–1688.
- Tunell, G. and Ksanda, C.J. (1936) The crystal structure of krennerite. *Journal of Washington Academy of Sciences*, 26, 509–528.
- Tunell, G. and Pauling, L. (1952) The atomic arrangement and bonds of the gold-silver ditellurides. *Acta Crystallographica*, 5, 375–381.
- Van Tendeloo, G. and Amelinckx, S. (1986) High-resolution electron-microscopic study of the modulated structure of kostovite ($\text{Cu}_{1-x}\text{Au}_{1+x}\text{Te}_4$). *Acta Crystallographica*, B42, 121–130.
- Van Tendeloo, G., Gregoriades, P., and Amelinckx, S. (1983a) Electron microscopy studies of modulated structures in $(\text{Au},\text{Ag})\text{Te}_2$: Part I. Calaverite AuTe_2 . *Journal of Solid State Chemistry*, 50, 321–334.
- (1983b) Electron microscopic studies of modulated structures in $(\text{Au},\text{Ag})\text{Te}_2$: Part II. Sylvanite AgAuTe_4 . *Journal of Solid State Chemistry*, 50, 335–361.
- Van Tendeloo, G., Amelinckx, S., and Gregoriades, P. (1984) Electron microscopic studies of modulated structures in $(\text{Au},\text{Ag})\text{Te}_2$: III. Krennerite. *Journal of Solid State Chemistry*, 53, 281–289.

MANUSCRIPT RECEIVED NOVEMBER 25, 2008

MANUSCRIPT ACCEPTED FEBRUARY 2, 2009

MANUSCRIPT HANDLED BY HONGWU XU